

# Joint Design of Low Sidelobe Radar Waveform and Filter with Hardware Platform Verification

Haoqian Rong\*, Shaojie Wang Zining Zhao Jiawei Zhang

\* School of Information Science and Engineering, YanShan University

Corresponding author: zhangjiw@ysu.edu.cn

**Abstract**— Radar waveform design is crucial for improving radar detection efficiency and accuracy. However, current theoretical research is disconnected from engineering practice, lacking verification in actual hardware systems. The paper first jointly designs radar waveforms and filters based on optimization theory to achieve range sidelobe suppression. Then, it constructs an arbitrary radar waveform transmitting/receiving platform using FPGA and high-speed AD modules, which can generate arbitrary waveforms, radiate them into space, receive target echo signals in an outdoor environment, and transmit them back to the host computer, thereby realizing real data verification of the waveform optimization algorithm. Corner reflectors are deployed as the targets to be measured in the real environment. The experimental results show that: each module of the hardware system functions as expected, with high accuracy in generating optimized waveforms and collecting signals; under the same bandwidth condition, the optimized waveforms have lower sidelobes compared to linear frequency modulation signals.

**Index Terms**—field programmable gate array(FPGA),analog to digital converter(AD),signal processing system

## I. SYSTEM ARCHITECTURE

The overall design of the radio transceiver system based on ADRV9009 and ZC706 is shown in Fig.1.

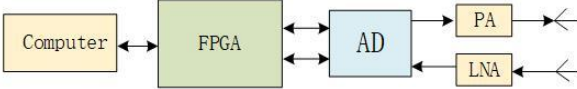


Fig. 1. The overall design of the radio transceiver system based on ADRV9009 and ZC706.

The hardware platform of the entire radio transceiver system consists of the following core components: ADRV9009 RF transceiver chip, AD9528 clock generator, Xilinx ZC706 FPGA development board, host computer control terminal, precision turntable, transmit power amplifier, and receive low-noise amplifier. As the core of the RF front-end, the ADRV9009's transmit chain upconverts the baseband waveform to the 5.5 GHz RF band for radiation, while the receive chain downconverts the captured RF signals to baseband through local oscillator mixing for digital signal processing by the FPGA. The AD9528 serves as the system clock source, providing synchronous reference clocks for both the ZC706 and ADRV9009.

Beyond the ADRV9009, the RF front-end integrates a 26 dB transmit power amplifier and a 30 dB receive low-noise amplifier to significantly enhance system dynamic range.

Both transmit and receive channels employ horn antennas

with 14 dB gain and 15° half-power beamwidth to ensure directional radiation and reception capabilities. The host computer controls the precision turntable carrying the antennas via the RS485 serial protocol, enabling precise angular scanning through customized command streams.

## II. LOW SIDELOBE WAVEFORM DESIGN

Considering a low-sidelobe waveform design, the objective function is selected as the integrated sidelobe level (ISL) of the correlation function between the waveform  $\mathbf{x} \in \mathcal{L}^N$  and the filter  $\mathbf{r} \in \mathcal{L}^N$ . The correlation function  $\mathbf{x}^H \mathbf{J}_r$  and  $\mathbf{r}^H \mathbf{J}_x$  are constructed using Toeplitz matrices  $\mathbf{J}_r$  and  $\mathbf{J}_x$ , with the matrices generated from  $r$  and  $x$ , respectively.

The ISL is given by

$$\text{ISL}(\mathbf{x}, \mathbf{r}) = \mathbf{x}^H \mathbf{J}_r \mathbf{W} \mathbf{J}_r^H \mathbf{x}$$

where  $\mathbf{W}$  is the sidelobe selection matrix, with ones on the diagonal at sample points corresponding to sidelobe regions and zeros elsewhere.

To guarantee the engineering applicability of the designed waveform, appropriate constraints are necessary. First, a constant modulus constraint is applied to maintain the radar amplifier in saturation mode and prevent amplitude modulation, given by  $\|x(i)\|^2 = 1, i = 1, K, N$ .

By synthesizing the objective function and constraint, the optimization problem is finally formulated as

$$P_0 \begin{cases} \min_{\mathbf{x}, \mathbf{r}} \mathbf{x}^H \mathbf{J}_r \mathbf{W} \mathbf{J}_r^H \mathbf{x} \\ \text{s.t.} \begin{cases} \|x(i)\|^2 = 1, i = 1, K, N \\ \mathbf{r}^H \mathbf{r} = \varepsilon \end{cases} \end{cases}$$

where  $\varepsilon$  is the energy of the filter.

The above problem is inherently NP-hard and intractable by conventional methods, thus requiring specialized solution strategies. First, a sequential variable

separation technique is applied to decompose  $P_0$  into a series of single-variable subproblems. With the introduction of iterative loop L1, the subproblem of  $\mathbf{x}$  at the  $k$ -th iteration, with the filter fixed at  $\mathbf{r} = \mathbf{r}^{(k-1)}$ , is formulated as

$$P_1 \begin{cases} \min_{\mathbf{x}} \mathbf{x}^H \mathbf{J}_{p^{(k-1)}} \mathbf{W} \mathbf{J}_{p^{(k-1)}} \mathbf{x} \\ \text{s.t.} \left\{ \|x(i)\|^2 = 1, i = 1, K, N \right. \end{cases}$$

Hence,  $P_1$  is convex in a single variable with the primary computational difficulty stemming from the constant modulus constraint. It can be addressed through power method-like iterations by solving  $P_1$ :

$$P_2 \begin{cases} \min_{\mathbf{x}^{(t+1)}} \|\mathbf{x}^{(t+1)} - \mathbf{T} \mathbf{x}^{(t)}\| \\ \text{s.t.} \left\{ \|x^{(t+1)}(i)\|^2 = 1, i = 1, K, N \right. \end{cases}$$

where  $\mathbf{T} = \lambda_{\max} \mathbf{I} - \mathbf{J}_{p^{(k-1)}} \mathbf{W} \mathbf{J}_{p^{(k-1)}}^H$ ,  $\lambda_{\max}$  is a constant greater than the maximum eigenvalue of  $\mathbf{J}_{p^{(k-1)}} \mathbf{W} \mathbf{J}_{p^{(k-1)}}^H$  and  $\mathbf{I}$  denotes the identity matrix. The solution to the subproblem of the filter is similar.

The iterative process alternately solves  $P_1$  and  $P_3$  in sequence, with termination triggered when the objective function ceases to exhibit significant improvement, i.e.,

$$ISL(\mathbf{x}^{(k-1)}, \mathbf{r}^{(k-1)}) - ISL(\mathbf{x}^{(k)}, \mathbf{r}^{(k)}) \leq \delta$$

where  $\delta$  is a small positive value.

### III. EXPERIMENT

In this experiment, we use the optimally designed waveform with a pulse width of 2  $\mu$ s and a bandwidth of 100 MHz. Fig 2 and 3 present the time-domain characteristics of the optimized waveform. The comparison of pulse compression results (Fig 5) indicates that after processing with the joint filter, the sidelobe envelope of the optimized waveform is significantly flattened, and the level of the first sidelobe is obviously lower than that of the LFM signal.

The transmitting end and receiving end of the ADRV9009 are connected with a radio frequency cable. Then, the waveform array is written into the FPGA to transmit and receive a low-sidelobe waveform, and then matched filtering is performed on the host computer. The hardware environment is shown in Fig. 4, and the matched filtering results are shown in Fig. 6.

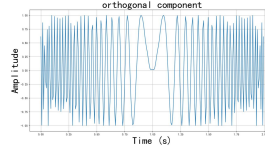


Fig. 2. in-phase component of the optimized waveform

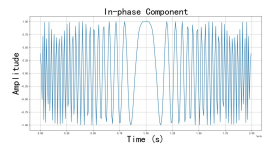


Fig. 3. quadrature component of the optimized waveform

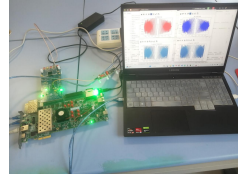


Fig. 4. Hardware environment

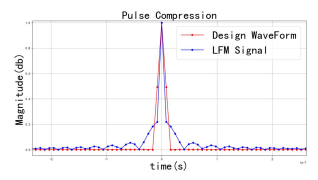


Fig. 5. Pulse compression between the optimized waveform and the chirp signal

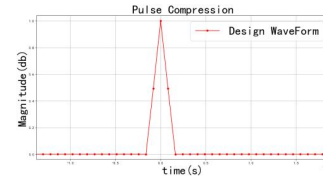


Fig. 6. matched filtering results

In the experiment, large and small corner reflectors were placed at distances of 9.6m and 14m, respectively. The imaging results are shown in Fig.9. It indicates that the main lobe of weak targets such as distant cars in the images formed by the designed waveform is not submerged under the sidelobes of strong targets, which proves that the designed waveform has lower sidelobes.



Fig. 7. outdoor experimental environment

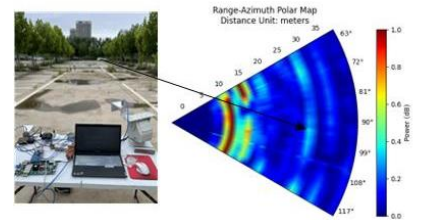


Fig. 8. Radar image formed by the low-sidelobe waveform

### IV. CONCLUSIONS

Based on the Xilinx ZC706 and ADRV9009 wideband RF front-end, this paper constructs an arbitrary radar waveform transceiver platform for verifying waveform optimization algorithms. Experimental observations show that the low-sidelobe waveform designed based on the optimized waveform theory achieves good imaging performance. Moreover, the designed waveform exhibits low sidelobes on the hardware platform. Future research can focus on synthetic aperture radar (SAR) imaging and verify the differences in imaging performance between traditional waveforms and low-sidelobe waveforms on this hardware platform.